Title

Pathological high frequency oscillations associate with increased GABA synaptic activity in pediatric epilepsy surgery patients.

Authors

Cepeda, Carlos
Levinson, Simon
Nariai, Hiroki
et al.

Publication Date

2020-02-01

DOI

10.1016/j.nbd.2019.104618

Peer reviewed

HHS Public Access

Author manuscript

Neurobiol Dis. Author manuscript; available in PMC 2021 February 01.

Published in final edited form as:

Neurobiol Dis. 2020 February ; 134: 104618. doi:10.1016/j.nbd.2019.104618.

Pathological High Frequency Oscillations Associate with Increased GABA Synaptic Activity in Pediatric Epilepsy Surgery Patients

Carlos Cepeda, PhD[1], **Simon Levinson, MD**[1], **Hiroki Nariai, MD**[4], **Vannah-Wila Yazon, BS**[1], **Conny Tran, MD**[1], **Joshua Barry, PhD**[1], **Katerina D. Oikonomou, PhD**[1], **Harry V. Vinters, MD**[3], **Aria Fallah, MD**[2], **Gary W. Mathern, MD**[1,2], **Joyce Y. Wu, MD**[4]

[1]IDDRC, Semel Institute for Neuroscience and Human Behavior, Mattel Children's Hospital, David Geffen School of Medicine at University of California Los Angeles, Los Angeles, CA, USA

[2]Department of Neurosurgery, Mattel Children's Hospital, David Geffen School of Medicine at University of California Los Angeles, Los Angeles, CA, USA

[3]Section of Neuropathology, Department of Pathology and Laboratory Medicine and Department of Neurology, Mattel Children's Hospital, David Geffen School of Medicine at University of California Los Angeles, Los Angeles, CA, USA

[4]Division of Pediatric Neurology, Mattel Children's Hospital, David Geffen School of Medicine at University of California Los Angeles, Los Angeles, CA, USA

Abstract

Pathological high-frequency oscillations (HFOs), specifically fast ripples (FRs, >250 Hz), are pathognomonic of an active epileptogenic zone. However, the origin of FRs remains unknown. Here we explored the correlation between FRs recorded with intraoperative pre-resection electrocorticography (ECoG) and spontaneous synaptic activity recorded *ex vivo* from cortical tissue samples resected for the treatment of pharmacoresistant epilepsy. The cohort included 47 children (ages 0.22-9.99 yr) with focal cortical dysplasias (CD types I and II), tuberous sclerosis complex (TSC) and non-CD pathologies. Whole-cell patch clamp recordings were obtained from pyramidal neurons and interneurons in cortical regions that were positive or negative for pathological HFOs, defined as FR band oscillations (250-500 Hz) at ECoG. The frequency of

Corresponding Author: Carlos Cepeda, Ph.D., IDDRC, Semel Institute for Neuroscience, Room 58-258, UCLA School of Medicine, 760 Westwood Plaza, Los Angeles, CA. 90024-1759, USA, ccepeda@mednet.ucla.edu, Tel: 310-206-0861; Fax: 310-206-5060.

Author Contributions

JYW and CC designed the experiments. GWM and AF performed the epilepsy surgeries. JYW and HN identified tissue samples as HFO+ or HFO−. HVV provided pathological interpretations. CC, KO and JB did the electrophysiological recordings in *ex vivo* slices. SL, CT, VWY analyzed spontaneous synaptic activity. CC, JYW, SL, GWM, HVV wrote the paper and all other authors reviewed and edited the manuscript.

Potential Conflicts of Interest

The authors declare no competing interests financial or otherwise.

Data Availability

The data that support the findings of this study are available from the corresponding author upon reasonable request.

spontaneous excitatory and inhibitory postsynaptic currents (sEPSCs and IPSCs, respectively) was compared between HFO+ and HFO− regions. Regardless of pathological substrate, regions positive for FRs displayed significantly increased frequencies of sIPSCs compared with regions negative for FRs. In contrast, the frequency of sEPSCs was similar in both regions. In about one third of cases (n=17), pacemaker GABA synaptic activity (PGA) was observed. In the vast majority (n=15), PGA occurred in HFO+ areas. Further, fast-spiking interneurons displayed signs of hyperexcitability exclusively in HFO+ areas. These results indicate that, in pediatric epilepsy patients, increased GABA synaptic activity is associated with interictal FRs in the epileptogenic zone and suggest an active role of GABAergic interneurons in the generation of pathological HFOs. Increased GABA synaptic activity could serve to dampen excessive excitability of cortical pyramidal neurons in the epileptogenic zone, but it could also promote neuronal network synchrony.

Keywords

Fast ripples; cortical dysplasia; GABA; electrophysiology; slice; synaptic activity

Introduction

It is generally assumed that an imbalance between excitation and inhibition underlies the generation of epileptic discharges (Dehghani et al., 2016; Weiss et al., 2019). Typically, increased glutamate receptor-mediated synaptic activity and/or reduced $GABA_A$ receptor-mediated synaptic activity are capable of facilitating epileptic activity. However, this rule is not universal. For example, a reduction of principal neuron firing caused by increased, synchronous GABAergic interneuron activity has been observed in association with low-voltage fast activity at the onset of focal seizures (de Curtis and Avoli, 2016). Further, during brain development GABA is depolarizing and, under certain conditions, excitatory (Ben-Ari, 2014; Ben-Ari, 2015). In previous studies we observed that in pediatric epilepsy cases, in particular those presenting with focal cortical dysplasia (FCD), spontaneous GABA synaptic activity was not reduced and in fact it was increased compared to glutamate activity (Cepeda et al., 2005). In addition, pacemaker GABA activity (PGA), consisting of rhythmic synaptic events, was frequently observed in FCD cases (Cepeda et al., 2014).

Interictal high frequency oscillations (HFO), specifically fast ripples (FR) in the range of 250-500 Hz, have been detected on intracranial ECoG and scalp EEG recordings in infants with epilepsy but not in normal controls, thus representing a *bona fide* marker of an active epileptic focus (Bernardo et al., 2018; Frauscher et al., 2017). FR detection is generally within or adjacent to the expected epileptogenic zone and rarely in distant “control” neocortex deemed not part of the epileptogenic zone by pre-surgical evaluation (Hussain et al., 2016; Kerber et al., 2014). In addition, complete resection of pathological cortical tissue presenting with FRs closely predicts postoperative seizure freedom in a number of clinical studies (Hussain et al., 2017; Jacobs et al., 2018; Jacobs et al., 2010; van ‘t Klooster et al., 2015; Wu et al., 2010b).

Although the neuronal and circuit substrates of physiological and pathological HFOs remain unknown, a parsimonious explanation suggested that multiple and diverse mechanisms are involved (Menendez de la Prida and Trevelyan, 2011). These include out-of-phase firing in neuronal clusters, excitatory AMPA receptor-mediated synaptic currents, and recurrent inhibitory connections in combination with fast time scales of inhibitory postsynaptic potentials, ephaptic, and interneuronal coupling through gap junctions (Bragin et al., 2002; Jefferys et al., 2012; Jiruska et al., 2017; Menendez de la Prida and Trevelyan, 2011; Staba and Bragin, 2011). While both pyramidal neurons and interneurons are involved in HFO generation, it is important to emphasize that *in vivo* recordings of human epileptic hippocampus demonstrated that pyramidal cells fre preferentially at the highest amplitude of the ripple (80-200 Hz), whereas interneurons begin to discharge earlier than pyramidal cells (Le Van Quyen et al., 2008). Further, mesial-temporal low-voltage fast (LVF) seizure onset in humans and animal models seems to result from increased inhibitory neuron firing that subsequently drives an increase in firing of excitatory neurons (Elahian et al., 2018; Shiri et al., 2015).

Considering the important role that interneuron activity plays in HFO and seizure generation, in the present electrophysiological study we examined the potential correlation between spontaneous GABA and glutamate synaptic activity of cortical pyramidal neurons (CPNs) with the presence or absence of intraoperative HFOs in *ex vivo* human tissue samples obtained from children with pharmaco-resistant seizures undergoing epilepsy neurosurgery.

Methods

Cohort and Standard Protocol Approvals:

The Institutional Review Board at UCLA approved the use of human subjects for research purposes, and parents or responsible persons signed written informed consents and HIPAA authorizations. Children undergoing resective surgery with the UCLA Pediatric Epilepsy Program to help control their medically refractory focal epilepsy were sequentially recruited from September 2007 to October 2017. This cohort includes the subset of children in our prospective HFO series whose intra-operative pre-resection ECoGs were analyzed visually for FR detection (Hussain et al., 2016). For the present study, cortical tissue samples from four groups of etiologies were included; CD type I, CD type IIa/b (Blumcke et al., 2011), Tuberous Sclerosis Complex (TSC), and non-CD etiologies including tumor, infarct, Sturge-Weber syndrome (SWS) and Rasmussen Encephalitis (RE).

Electrocorticography and Surgical Resection:

The site and margin of the surgical resection were based on recommendations from a multidisciplinary meeting after careful consideration of the presurgical evaluation of each patient, as previously described (Cepeda et al., 2003). For all 4 groups of etiologies, our goal was complete resection of the epileptogenic zone primarily defined by non-invasive testing (Hemb et al., 2010; Lerner et al., 2009; Salamon et al., 2008; Wu et al., 2010a), including video-EEG capturing ictal events, high-resolution MRI and 18-Fluorodeoxyglucose positron emission tomography (FDG-PET), as well as magnetic source imaging (Wu et al., 2006) and

co-registration of MRI and FDG-PET when the initial battery of tests was inconclusive (Salamon et al., 2008).

In the operating room, we routinely utilized brief intraoperative pre-resection ECoG to confirm and/or refine the ultimate margins of the surgical resection site. With this brief intraoperative ECoG, HFOs, specifically the FR bandwidth (250-500 Hz), were identified in the operating room as soon as recording ended but before resection began as previously described (Hussain et al., 2016; Wu et al., 2010b). FR localization was not performed as a clinical trial and therefore did not affect surgical resection for any of the patients.

Electrocorticography recording and visual analysis of HFOs:

ECoG recordings were obtained using Harmonie long-term monitoring system (Stellte/Alpine Biomed; Montreal, Canada) between 2007-2014, and Nihon Kohden long-term monitoring system (Irvine, California, USA) between 2014-2017 using grid macroelectrodes as clinically indicated. ECoG was acquired with a digital sampling frequency of 2000 Hz, which defaults to a setting of a low-frequency filter of 0.016 Hz and a high-frequency filter of 600 Hz at the time of acquisition. For intra-operative pre-resection ECoG samples, the anesthesia was standardized so that patients were maintained on narcotics and paralytic agents, and a minimum of 10 min was recorded after sevoflurane and propofol discontinuation to mitigate any anesthetic effects on the ECoG (Hussain et al., 2016; Wu et al., 2010b). With the default EEG reviewing software settings provided by each vendor, conventional epileptiform discharges (e.g., spikes, paroxysmal fast activity) were marked with standard review settings (30 mm/sec; high-pass filter = 1 Hz; low-pass filter = 70 Hz; notch filter = 60 Hz). FRs were reviewed and marked in a side-by-side fashion such that standard ECoG (settings as above) were displayed on the left side, and HFOs were displayed (and time-locked) on the right side. FRs were viewed with 300 mm/sec, bandpass filter 250-500 Hz (see examples in Fig. 1). Supplementary Fig. 1 shows the electrode montage for the cases illustrated in Fig. 1 (upper panel). Inclusion criteria for FRs included; oscillatory events with at least four cycles, which were clearly visible above the background signal in the filtered data and at least twice the voltage amplitude. Exclusion criteria included; any potential fast activity that could be spurious was considered an artifact. Other potential artifacts such as DC shift, electrode movement or manipulation in the surgical field, pulse artifact, known non-recording electrode due to its position over encephalomalacia or not directly over cortex. Once FRs had been identified, they were further localized on the intra-operative pre-resection ECoG to a specific cortical region. The FR identification and localization were completed within 5-10 minutes, and were timed to correspond with the neurosurgical activities in the operating room to minimize prolonging the surgical time unnecessarily.

At a later stage, outside the operating room, time-frequency analysis of FRs was performed using BESA EEG software (MEGIS Software GmbH, Grafelfng, Germany) and based on the same analysis approaches reported in prior studies (Nariai et al., 2011a; Nariai et al., 2011b). We analyzed putative events from −500 and +500 ms in 10 ms bins and between 10600 Hz in 5 Hz bins to visualize and quantify FRs. We confirmed there was a significant augmentation (>100% increase in amplitude compared to the baseline period between −500

ms and −400 ms) of isolated FR band (250-500 Hz) activity, which lasted longer than four cycles. Additionally, we confirmed that visually marked events were not artifacts. This analysis further validated the visually identified FR events.

The cortical tissue displaying FR generation (HFO+) was considered the most epileptogenic portion of the total resection. Tissue that was part of the planned resection but did not display FRs (HFO−) was used for comparison. Experimenters received 1 or 2 samples, and were blind as to which sample was HFO+ and which sample was HFO−. Both tissue samples were processed similarly. The identity of the samples was revealed by the neurosurgeon only after the experimenters completed their analyses.

Specimen Transport, Slice Preparation, and Electrophysiological Recordings:

The HFO+ and HFO− samples, i.e., with and without FRs, were resected with no use of electrocautery. The tissue samples were immediately immersed in ice-cold artificial cerebrospinal fluid (ACSF) enriched with sucrose for better preservation and then expeditiously hand-carried out of the operating room and transported directly to the laboratory within 5-10 min after resection. The high sucrose-based slicing solution contained (in mM): 26 $NaHCO_3$, 1.25 NaH_2PO_4, 208 sucrose, 10 glucose, 2.5 KCl, 1.3 $MgCl_2$, 8 $MgSO_4$. Coronal slices (300 μm) were cut and transferred to an incubating chamber containing ACSF (in mM): 130 NaCl, 3 KCl, 1.25 NaH_2PO_4, 26 $NaHCO_3$, 2 $MgCl_2$, 2 $CaCl_2$, and 10 glucose) oxygenated with 95% O_2-5% CO_2 (pH 7.2-7.4, osmolality 290-310 mOsm/L, 32-34°C). Slices were allowed to recover for an additional 60 min at room temperature prior to recording. All recordings were performed at room temperature using an upright microscope (Olympus BX51WI) equipped with infrared-differential interference contrast (IR-DIC) optics.

Whole-cell patch clamp recordings in voltage- or current-clamp modes were obtained from CPNs (layers II-V) visualized with IR-DIC (Cepeda et al., 2012). The patch pipette (3-5 MΩ resistance) contained a cesium-based internal solution (in mM): 125 Cs-methanesulfonate, 4 NaCl, 1 $MgCl_2$, 5 MgATP, 9 EGTA, 8 HEPES, 1 GTP-Tris, 10 phosphocreatine, and 0.1 leupeptin (pH 7.2 with CsOH, 270-280 mOsm/L) for voltage clamp recordings. K-gluconate-based solution containing (in mM): 112.5 K-gluconate, 4 NaCl, 17.5 KCl, 0.5 $CaCl_2$, 1 $MgCl_2$, 5 ATP, 1 NaGTP, 5 EGTA, 10 HEPES, pH 7.2 (270–280 mOsm/L) was used for current clamp recordings. After breaking the seal, basic cell properties (membrane capacitance, input resistance, decay time constant) were recorded while holding the membrane potential at −70 mV. Electrode access resistances during whole-cell recordings were less than 25 MΩ (range 8-25 MΩ).

In voltage clamp mode, spontaneous excitatory and inhibitory post-synaptic currents (sEPSCs and sIPSCs) were measured. Three investigators blinded to the tissue origin and whether the recording was from a neuron in the HFO+ or HFO− area assisted in electrophysiological data analysis. Frequency of spontaneous synaptic currents was assessed using MiniAnalysis software (Synaptosoft). The values obtained by each investigator were averaged. Electrophysiological findings were then correlated with the 4 groups of etiologies mentioned above, namely CD types land IIa/b, TSC, and non-CD etiologies.

Statistics:

In the text and figures, results are expressed as mean±SEM. For group comparisons, we used one-way ANOVA (with Bonferroni correction) or ANOVA of Ranks (Dunn's method) tests. For simple comparisons between 2 groups we used the Student's *t* test and for comparisons between proportions the Chi-square test was used. SigmaStat (3.5) software was used for all statistical tests. Differences were deemed statistically significant if $p<0.05$.

Results

Cohort:

The cohort in this study included 47 pediatric epilepsy cases (28 males and 19 females), most with CD types I (n=13) and IIa/b (n=15), TSC (n=10), and non-CD etiologies (n=9) including infarct (n=5), tumor (n=1), RE (n=1), SWD (n=1) and polymicrogyria (n=1) (Table 1). The mean age of the patients was 3.3±1.7 years. No significant age differences were found among those with the different pathological substrates or between HFO+ and HFO− samples ($p=0.34$, one-way ANOVA). Supplementary Table 1 shows in more detail the cohort examined, age, gender, and number of cells recorded in HFO+ and HFO− samples. At the time of surgery, patients had been treated pharmacologically with antiepileptic drugs that included topiramate, phenobarbital, lamotrigine, zonisamide, clonazepam, carbamazepine and adrenocorticotropic hormone.

The methodology for identifying and localizing FRs was strictly followed as described above. All visually identified FR episodes in the operating room were retrospectively validated with computer-based time-frequency analysis. The frequency range of HFOs in our cohort oscillated between 250 and 500 Hz. The median frequency at highest amplitude was 320 Hz (range: 250-390 Hz) and the median duration of the FRs was 42.5 ms (range: 25-50 ms) (Fig. 1).

In a subset of pediatric epilepsy surgery patients (n=30) that included some of the cases examined in the present study we quantified the association between FRs and other paroxysmal events and found that FRs were accompanied by interictal spikes in 22% of cases, by sharp waves in 11%, by background voltage attenuation in 2%, and by paroxysmal fast activity in 1%. FRs occurred independently of other EEG findings in 64% of recorded FR events (Wu et al., 2010b). Based on the same study the FR rate was 1.23/min on average.

Pathologic Findings:

In patients with CD type I (n=13) and type II (n=15) histological analyses revealed changes consistent with the ILAE consensus classification of FCDs (Blumcke et al., 2011). In CD type I these included moderate to severe neuronal disorganization, heterotopic neurons in the white matter, mild neuronal crowding and, in some cases, blurring of the gray-white matter junction. In patients with CD type II, in addition to neuronal disorganization, dysmorphic, cytomegalic neurons (IIa) and balloon cells (IIb) also occurred. TSC cases (n=10) displayed giant cells and dysmorphic cytomegalic neurons. Severe neuronal disorganization and heterotopic neurons in the white matter were also observed. In infarct cases (n=5), two patients had a cystic infarct with gliosis, two other patients had some neuronal crowding but

no evidence of dyslamination, while the remaining patient had some scattered heterotopic neurons in the white matter. The RE case showed multifocal, variably severe reactive gliosis, areas of perivascular cuffing by mononuclear inflammatory cells, and capillary proliferation. The SWS case showed pronounced leptomeningeal angiomatosis, with predominantly thin-walled, venous channels. The tumor case had a small oligodendroglial hamartoma and the remaining case presented with polymicrogyria and pachygyria.

Basic cell membrane properties:

In the present cohort, a total of 201 pyramidal neurons were recorded, 145 cells were in samples displaying HFOs during the intraoperative ECoG recordings and 56 were from HFO − samples. These numbers were expected as HFO+ areas usually overlap with the pathological substrate (Hussain et al., 2016) and the area of planned resection. Cells in the HFO− areas were either adjacent to HFO+ areas or in a different cortical region. The neurons were most often from the frontal (n=103) and temporal (n=75) areas, with a few additional cells found in the parietal (n=21) and occipital (n=2) lobes.

Pyramidal neuron membrane properties were estimated in voltage clamp recordings using a Cs^+-based internal solution. Pyramidal neurons were divided into two groups based on their location in HFO+ and HFO− cortical areas (Fig. 2). There was no significant difference in mean cell membrane capacitance in HFO+ (n=145) compared with HFO− (n=56) areas (p=0.359, Student's t-test). In contrast, cell membrane input resistance was significantly reduced in HFO+ compared with HFO− areas (p=0.025, Student's t-test). The decay time constant was indistinguishable in the two groups (p=0.649). The percentage of cytomegalic neurons, identified based on measurements of cell capacitance and biocytin staining (Cepeda et al., 2003), was higher in HFO+ (23/145, 15.9%) compared with HFO− (5/56, 8.9%) areas. However, this difference was not statistically significant (p= 0.2, Chi-square).

The frequency of sIPSCs was increased in HFO+ versus HFO− areas and across pathologies:

First we determined the frequency of sIPSCs in HFO+ versus HFO− areas in the four pathologies combined. As previously reported, sIPSCs in our recording conditions are mediated by $GABA_A$ receptors as they are completely abolished with bicuculline (Cepeda et al., 2014). The frequency of sIPSCs for cells from the HFO+ group was significantly higher than that from the HFO− group, with mean frequencies of 10.07±0.56 Hz and 4.46±0.43 Hz ($p<0.001$, t-test), respectively (Fig. 3A**, left panel)**. Similarly, across all pathological groups investigated (CD type I, CD type IIa/b, TSC and non-CD), HFO+ samples had a significantly higher sIPSC frequency than HFO− samples (Fig. 3A**, right panel)**. Twenty-two tissue samples from 13 patients were classified as CD type I. In total, 63 cells were recorded [frontal (n=42), temporal (n=9), parietal (n=12)]. The mean IPSC frequency in pyramidal neurons from HFO+ areas in patients with CD type I was higher than in cells from HFO− areas ($p<0.012$). Nineteen samples were classified as either CD type IIa or IIb (15 patients). In total, 55 cells were recorded [frontal (n=24), temporal (n=27), parietal (n=4)]. IPSC frequency was higher in cells from HFO+ than in cells from HFO− areas ($p<0.002$). The patient with dual pathology (CD type IIa and Rasmussen's encephalitis) was included in this group. A single sample was obtained from this patient (frontal) and 5 cells

were recorded. In the 10 patients with TSC, 12 samples were examined. In total, 39 cells were recorded [frontal (n=27), parietal (n=10), occipital (n=2)]. Again, the frequency of IPSCs was higher in HFO+ samples (p=0.043). In the non-CD group with a history of infarct or stroke (5 patients), 6 samples were obtained. We examined 27 cells [temporal (n=21) and frontal (n=6)]. In the Rasmussen's Encephalitis case two tissue samples were obtained and 3 cells (frontal) were recorded. In the Sturge-Weber case, 2 tissue samples were examined. All cells (n=7) were from the temporal region. In the tumor case, 2 cells were recorded in the frontal resection. Finally, in the polymicrogyria/pachygyria case, 5 cells from the frontal region were recorded. As in the other groups, in the non-CD group the frequency ofIPSCs was increased in HFO+ compared with HFO− areas ($p<0.001$).

Comparison of sIPSC frequency in HFO+ versus HFO− areas within the same patient:

The difference in frequency also was evident when 2 samples (one positive and one negative for HFOs) from the same patient were compared side by side (Fig. 3B). Ten cases met this criterion and a total of 58 cells (32 HFO+ and 26 HFO−) were analyzed and were also included in the larger analysis above. There were 4 CD type I patients (26 cells: 20 frontal, 4 parietal, 2 temporal), 3 CDII patients (12 cells: 3 frontal, 9 temporal), 1 TSC patient (9 cells: 3 frontal, 6 parietal), 1 infarct patient (6 cells: 3 frontal, 3 temporal) and 1 patient with polymicrogyria (5 cells: 3 frontal, 2 parietal). Across all pathologies, the frequency of sIPSCs was significantly greater in HFO+ than in HFO− negative areas ($p<0.001$). In no case was the mean sIPSC in HFO+ areas less than the mean sIPSC frequency in HFO− areas **(see** Supplementary Fig. 2). Two illustrative cases from a CD type I and a stroke patient are shown in Fig. 4 A, B.

Pathological HFOs also are associated with pacemaker GABA synaptic activity in CD, TSC, and non-CD cases:

Previous stereo-EEG recordings demonstrated the occurrence of rhythmic spike discharges in the epileptogenic zone corresponding to histologically defined FCD cases (Chassoux et al., 2000; Gambardella et al., 1996). In our *in vitro* studies we found that in many CD cases (~30%), and a smaller percentage of non-CD cases (~10%), spontaneous pacemaker GABA synaptic activity (PGA) also occurred and hypothesized that PGA was the cellular substrate of rhythmic epileptic discharges observed with EEG recordings (Cepeda et al., 2014). PGA is action potential-dependent as it is abolished when Na^+ channels are blocked with tetrodotoxin (TTX) and is exacerbated in the presence of the K^+ channel blocker 4-aminopyridine (4-AP, 100 μM) (Fig. 5A, B). In the present cohort, PGA in the form of either continuous or episodic rhythmic synaptic events (5-10 Hz), was observed in 36% of cases (17/47; 7 with CDI, 4 with CDII, 3 with TSC, and 3 with non-CD pathologies). Of the 17 cases displaying PGA, 15 cases were HFO+ and only 2 were HFO−, suggesting a tight association between the occurrence of PGA and pathological HFOs. In a subset of cases (n=7), we were able to compare the association between PGA and HFOs in two samples obtained from the same patient. PGA was observed in 6 samples that were classified as HFO + and in only 1 sample classified as HFO−, further supporting the close association between HFOs and PGA.

Interneuron activity in HFO+ areas is increased:

Among other mechanisms, GABAergic interneurons, in particular fast-spiking interneurons (FSIs) expressing parvalbumin, have been proposed as potential generators of HFOs. A small number of interneurons were recorded in HFO+ (n=28, 21 cases) and HFO− (n=7, 5 cases) areas. Interneurons were easily identified by their unique passive and active cell membrane properties as well as, in some cases, by biocytin labeling (Fig. 6A). Compared with pyramidal neurons, interneuron cell membrane capacitance was significantly lower, input resistance was higher and decay time constant was faster. This was true regardless of the location of interneurons in HFO+ versus HFO− areas. However, comparison of the basic membrane properties of interneurons located in HFO+ versus HFO− areas revealed no significant differences (Table 2). A reliable measure of cellular excitability is the ability to generate action potentials. If interneuron firing is increased, this could explain increased frequency of sIPSCs. Indeed, estimates of interneuron firing demonstrated significantly higher firing rates of interneurons in HFO+ (n=26) versus those in HFO− (n=3) areas (average 103±10 Hz and 60±6 Hz respectively and a median of 87 Hz and 60 Hz, p=0.03, Mann-Whitney Rank Sum Test). In addition, about half of the interneurons in HFO+ areas displayed signs of hyperexcitability whereas interneurons in HFO− areas did not. This hyperexcitability was manifested by spontaneous, recurrent ictal-like discharges (~12 sec duration) (Fig. 6B), faster and prolonged action potential firing (Fig. 6C), and the occurrence of slowly- and non-inactivating spikelets during slowly depolarizing ramp voltage commands (Fig. 6D).

The frequency of sEPSCs is similar in HFO+ versus HFO− areas:

Increased excitability of pyramidal neurons could also contribute to the generation of pathological HFOs. If this is the case, one could expect increased sEPSC frequency. However, quantification of sEPSC frequency did not support this hypothesis. Pyramidal neurons from HFO+ and HFO− areas had similar average sEPSC frequencies. Thirty-one cells [CD type I (n=8), CD type II (n=9), TSC (n=7), Non-CD (n=7)] were analyzed with 17 coming from HFO+ samples and 14 from HFO− samples. These cells were a subset of the cells analyzed for IPSCs. The mean EPSC frequency of cells recorded in HFO+ areas was 2.52±0.38 Hz and the mean frequency in HFO− areas was 2.44±0.49 Hz (p=0.58) (Fig. 7). We obtained similar results when sEPSC frequencies of pyramidal cells in HFO+ and HFO− samples from the same patients (n=6) were compared. In cells from HFO+ areas average frequency was 2.83±0.5 Hz (n=10) and in cells from HFO− areas the average frequency was 2.1±0.5 Hz (n=13). The difference was not statistically significant (p=0.41).

Despite the lack of significant differences in the frequency of sEPSCs, which reflect the level of pyramidal neuron activity, we also looked for signs of CPN hyperexcitability. Only 3 out of 201 neurons (1.5%) displayed signs of hyperexcitability. In voltage clamp mode, upon a slowly depolarizing ramp voltage command and similar to FSIs, these cells displayed high-frequency spikelets (Fig. 8). All cells were found in HFO+ areas, whereas no cells from HFO− areas were found. This suggests that in our cohort, HFOs were most likely instigated by GABAergic interneurons.

Discussion

Ever since the recognition of HFOs, in particular FRs, as a *bona fide* surrogate marker of epileptogenic networks (Bragin et al., 1999; Bragin et al., 2002; Jacobs et al., 2012; Jozwiak et al., 2017), the search for a possible generator of HFOs began. However, to date, the cellular basis for this type of pathological oscillation has remained unclear. In this study, using patch clamp electrophysiological recordings in slices identified as derived from HFO+ or HFO− cortical tissue samples, we demonstrate a close association between HFO+ areas and increased frequency of sIPSCs. HFO+ areas also correlated with pyramidal neurons displaying PGA, a cellular substrate of rhythmic epileptic discharges. In addition, GABA interneurons in HFO+ areas displayed signs of hyperexcitability manifested by increased firing frequencies and the presence of ictal-like discharges. These results support an important role for GABA networks in the generation of pathological HFOs in substrates like CD, TSC and non-CD etiologies in pediatric epilepsy surgery patients.

Our cohort of pediatric epilepsy patients (average 3.3±1.7 yr of age) included four main types of pathologies; CD type I, CD type II, TSC, and a variety of non-CD pathologies. More patients presented with FCD compared with any other group. This was not surprising as CD is the most common (>50%) pathological substrate in epilepsy surgery patients under 5 years of age operated in our institution (Hemb et al., 2010; Lerner et al., 2009). A previous study analyzing the rates of HFOs (80-450 Hz) in mostly adult patients with pathologically confirmed FCD type 1 compared with those with type 2 showed that patients with FCD type 2 had significantly higher rates of HFOs than patients with FCD type 1, thereby mirroring the higher epileptogenicity of FCD type 2 compared with FCD type 1 lesions (Kerber et al., 2013). Cases with non-CD pathologies tended to be older but the age difference was not statistically significant in our study. As the primary goal of epilepsy surgery is the removal of the epileptogenic zone in order to render the patient seizure-free, not surprisingly more samples and neurons were collected in HFO+ than in HFO− areas. This was particularly true for TSC cases, where HFO− samples were difficult to obtain. In spite of this caveat, important differences in membrane properties and GABA synaptic activity were observed.

There was a slight trend for larger average cell capacitance in HFO+ areas and a statistically significant reduction in average input resistance of pyramidal neurons from HFO+ areas. As dysmorphic, cytomegalic pyramidal neurons are more commonly found in the most anatomically abnormal areas (also corresponding to HFO+ areas) of CD and TSC cases, it was expected that overall cell capacitance would be increased and input resistance decreased. This was not the case, probably because in those same areas immature pyramidal neurons also are found, generating great variability in cell capacitance and input resistance measures (Cepeda et al., 2007). However, decreases in cell membrane input resistance in HFO+ areas were statistically significant, suggesting that other factors besides membrane area could influence input resistance, e.g., more gap junctions in HFO+ areas, which could also contribute to the generation of HFOs (Jefferys et al., 2012).

Regardless of pathological substrate, HFOs were associated with increased spontaneous GABA synaptic activity. This indicates that the presence of HFOs is not determined by the underlying pathologic lesion but by a common microcircuit functional abnormality,

consistent with previous findings (Jacobs et al., 2009). HFOs also were associated with the presence of PGA (Cepeda et al., 2014), a rhythmic pattern of $GABA_A$ receptor-mediated synaptic activity that could explain the occurrence of rhythmic epileptic discharges frequently observed in FCD cases (Chassoux et al., 2000; Gambardella et al., 1996). These findings suggest that GABA interneurons could play an important role in the generation of pathological HFOs. Consistent with this hypothesis, we found that GABA interneurons, identified by typical biophysical membrane properties and biocytin staining, displayed signs of hyperexcitability which included increased firing rates, ictal-like discharges, as well as slowly- and non-inactivating Na^+ spikelets. These spikelets have been suggested to reflect the occurrence of ectopic axonal or dendritic spikes (Epsztein et al., 2010; Michalikova et al., 2017; Pinato and Midtgaard, 2005) and in the 4-AP epilepsy model they signal increased excitability of axonal terminals associated with synchronous GABA-mediated potentials (Avoli et al., 1998). Spikelets may also reflect the presence of gap junctions (Mercer et al., 2006; Vigmond et al., 1997; Zsiros and Maccaferri, 2005), which are involved in HFO generation and neuronal synchrony. Nonetheless, while GABA interneurons appear to play a key role in pathological HFO generation, other factors cannot be ruled out. It is generally accepted that FRs are generated by synchronous or out-of-phase firing of principal neurons (Bragin et al., 2011; Jefferys et al., 2012; Jiruska et al., 2017; Menendez de la Prida and Trevelyan, 2011). However, the role of GABAergic interneurons in pathological FR generation is not well understood. In fact, it has been shown that during the buildup phase PV interneurons discharge at very high rates leading to depolarization block, which results in synchronous firing of pyramidal neurons (Gulyas and Freund, 2015). Interestingly, at least in our pediatric cohort, glutamatergic synaptic activity did not seem to be affected, although on rare occasions pyramidal neurons also displayed signs of hyperexcitability.

Our findings are in line with a study on the spontaneous emergence of seizure-like events in juvenile rat hippocampal slices bathed in low-Mg^{2+}, which demonstrated that GABAergic synaptic currents in pyramidal cells coincided with HFOs (400-800 Hz), whereas the glutamatergic input lagged by approximately 10 ms (Lasztoczi et al., 2009). This suggested that GABAergic input contributes to synchronization and recruitment of pyramidal cells. Further, in an *in vitro* 4-AP model in conjunction with optogenetic control of parvalbumin-positive interneurons in the entorhinal cortex, it was found that LVF-onset seizure patterns presented with higher ripple than fast ripple rates, demonstrating the involvement of interneuronal networks in seizure onset (Shiri et al., 2015). Also in the 4-AP seizure model, interneuronal network activity was shown to precede seizure activity, supporting an important role of GABA interneurons in focal seizure generation (Librizzi et al., 2017). Consistent with this idea, in humans mesial-temporal LVF seizure onset appears to result from increased inhibitory neuron firing (Elahian et al., 2018). Studies in pediatric CD tissue have demonstrated that GABA neurotransmission, including PGA, can depolarize immature pyramidal neurons (Cepeda et al., 2007) and, in fact, seems to underlie spontaneous interictal discharges due to altered chloride cotransporter expression and paradoxical depolarization of pyramidal neurons (Blauwblomme et al., 2019). Thus, GABAergic interneurons can provide excitatory drive to epileptic circuits *via* distinct neurological mechanisms (Ye and Kaszuba, 2017), particularly during early development (Le Van Quyen et al., 2006).

One potential limitation of our study is that brain tissue samples were categorized based on the presence or absence of FRs (250-500 Hz). This was done on the assumption that FRs, more than physiological ripples (80-250 Hz), specifically localize in epileptogenic regions (Jacobs et al., 2010; van ‘t Klooster et al., 2017). However, a recent study demonstrated very rare (0.038/min) FRs in normal brain regions (Frauscher et al., 2018). Although there is a slim possibility that some FRs were indeed physiological, the presence of FRs remains a specific marker for the epileptogenic zone, particularly when supported by multimodal information including seizure semiology, non-invasive video-EEG monitoring, neuroimaging, and traditional ECoG recordings. Another potential limitation of our study is that there was no confirmation that slices from the resected tissue generated FRs. We opted to categorize the samples based on the *in vivo* ECoG recordings to avoid false negatives, e.g., absence of FRs due to lack of long range excitatory inputs, or false positives, e.g., presence of FRs caused by the trauma during and after the slicing procedure.

Conclusions

Regardless of pathology, the frequency of sIPSCs recorded from CPNs was significantly higher in tissue samples displaying pathological HFOs. Further, if HFOs were observed in two different cortical areas in the same patient, the increase was more dramatic in areas with the greatest structural abnormality based on MRI. This suggested that GABAergic interneurons are hyperactive in areas with HFOs and could play an active role in FRs generation and network synchronization. This was indeed the case as FSIs displayed signs of hyperexcitability. While the most accepted canon is that FRs emerge from synchronous activation of CPNs, we hypothesize that FSIs could directly contribute to pathological FR generation. We also demonstrated that FR areas not only correlate with high GABA synaptic activity but also with the PGA we described several years ago (Cepeda et al., 2014). This is significant because EEG studies in FCD have shown that rhythmic epileptic discharges (REDs) associate with the structural abnormalities in the epileptogenic region and we showed that PGA could in fact underlie REDs (Cepeda et al., 2014; Chassoux et al., 2000; Gambardella et al., 1996). From a clinical perspective, our results suggest that selective modulation of GABA interneuron activity, in particular FSIs, could have a profound impact on HFO generation and spontaneous seizure occurrence.

Supplementary Material

Refer to Web version on PubMed Central for supplementary material.

Acknowledgments

We deeply appreciate the patients and their parents for allowing the use of resected specimens for experimentation. We also thank the UCLA Hospital Pediatric Neurology staff for their assistance and dedication. Dr. Anatol Bragin provided helpful comments and insights on the manuscript. Ms. My N. Huynh performed the biocytin processing. This study was supported by NIH grant NS082649 (JYW).

References

Avoli M, et al., 1998 GABA-dependent generation of ectopic action potentials in the rat hippocampus. Eur J Neurosci. 10, 2714–22. [PubMed: 9767401]

Ben-Ari Y, 2014 The GABA excitatory/inhibitory developmental sequence: a personal journey. Neuroscience. 279, 187–219. [PubMed: 25168736]

Ben-Ari Y, 2015 Commentary: GABA depolarizes immature neurons and inhibits network activity in the neonatal neocortex in vivo. Front Cell Neurosci. 9, 478. [PubMed: 26733806]

Bernardo D, et al., 2018 Visual and semi-automatic non-invasive detection of interictal fast ripples: A potential biomarker of epilepsy in children with tuberous sclerosis complex. Clin Neurophysiol. 129, 1458–1466. [PubMed: 29673547]

Blauwblomme T, et al., 2019 Gamma-aminobutyric acidergic transmission underlies interictal epileptogenicity in pediatric focal cortical dysplasia. Ann Neurol. 85, 204–217. [PubMed: 30597612]

Blumcke I, et al., 2011 The clinicopathologic spectrum of focal cortical dysplasias: a consensus classification proposed by an ad hoc Task Force of the ILAE Diagnostic Methods Commission. Epilepsia. 52, 158–74. [PubMed: 21219302]

Bragin A, et al., 2011 Further evidence that pathologic high-frequency oscillations are bursts of population spikes derived from recordings of identified cells in dentate gyrus. Epilepsia. 52, 45–52.

Bragin A, et al., 1999 High-frequency oscillations in human brain. Hippocampus. 9, 137–42. [PubMed: 10226774]

Bragin A, et al., 2002 Local generation of fast ripples in epileptic brain. J Neurosci. 22, 2012–21. [PubMed: 11880532]

Cepeda C, et al., 2005 Pediatric cortical dysplasia: correlations between neuroimaging, electrophysiology and location of cytomegalic neurons and balloon cells and glutamate/GABA synaptic circuits. Dev Neurosci. 27, 59–76. [PubMed: 15886485]

Cepeda C, et al., 2012 Enhanced GABAergic network and receptor function in pediatric cortical dysplasia Type IIB compared with Tuberous Sclerosis Complex. Neurobiol Dis. 45, 310–21. [PubMed: 21889982]

Cepeda C, et al., 2007 Immature neurons and GABA networks may contribute to epileptogenesis in pediatric cortical dysplasia. Epilepsia. 48 Suppl 5, 79–85. [PubMed: 17910585]

Cepeda C, et al., 2014 Pacemaker GABA synaptic activity may contribute to network synchronization in pediatric cortical dysplasia. Neurobiol Dis. 62, 208–17. [PubMed: 24121115]

Cepeda C, et al., 2003 Morphological and electrophysiological characterization of abnormal cell types in pediatric cortical dysplasia. J Neurosci Res. 72, 472–86. [PubMed: 12704809]

Chassoux F, et al., 2000 Stereoelectroencephalography in focal cortical dysplasia: a 3D approach to delineating the dysplastic cortex. Brain. 123 (Pt 8), 1733–51. [PubMed: 10908202]

de Curtis M, Avoli M, 2016 GABAergic networks jump-start focal seizures. Epilepsia. 57, 679–87. [PubMed: 27061793]

Dehghani N, et al., 2016 Dynamic Balance of Excitation and Inhibition in Human and Monkey Neocortex. Sci Rep. 6, 23176. [PubMed: 26980663]

Elahian B, et al., 2018 Low-voltage fast seizures in humans begin with increased interneuron firing. Ann Neurol. 84, 588–600. [PubMed: 30179277]

Epsztein J, et al., 2010 Impact of spikelets on hippocampal CA1 pyramidal cell activity during spatial exploration. Science. 327, 474–7. [PubMed: 20093475]

Frauscher B, et al., 2017 High-frequency oscillations: The state of clinical research. Epilepsia. 58, 1316–1329. [PubMed: 28666056]

Frauscher B, et al., 2018 High-Frequency Oscillations in the Normal Human Brain. Ann Neurol. 84, 374–385. [PubMed: 30051505]

Gambardella A, et al., 1996 Usefulness of focal rhythmic discharges on scalp EEG of patients with focal cortical dysplasia and intractable epilepsy. Electroencephalogr Clin Neurophysiol. 98, 243–9. [PubMed: 8641147]

Gulyas AI, Freund TT, 2015 Generation of physiological and pathological high frequency oscillations: the role of perisomatic inhibition in sharp-wave ripple and interictal spike generation. Curr Opin Neurobiol. 31,26–32. [PubMed: 25128735]

Hemb M, et al., 2010 Improved outcomes in pediatric epilepsy surgery: the UCLA experience, 1986–2008. Neurology. 74, 1768–75. [PubMed: 20427752]

Hussain SA, et al., 2017 Intraoperative fast ripples independently predict postsurgical epilepsy outcome: Comparison with other electrocorticographic phenomena. Epilepsy Res. 135, 79–86. [PubMed: 28644979]

Hussain SA, et al., 2016 Prospective and “live” fast ripple detection and localization in the operating room: Impact on epilepsy surgery outcomes in children. Epilepsy Res. 127, 344–351. [PubMed: 27721161]

Jacobs J, et al., 2009 High frequency oscillations in intracranial EEGs mark epileptogenicity rather than lesion type. Brain. 132, 1022–37. [PubMed: 19297507]

Jacobs J, et al., 2012 High-frequency oscillations (HFOs) in clinical epilepsy. Prog Neurobiol. 98, 302–15. [PubMed: 22480752]

Jacobs J, et al., 2018 Removing high-frequency oscillations: A prospective multicenter study on seizure outcome. Neurology. 91 , e1040–e1052. [PubMed: 30120133]

Jacobs J, et al., 2010 High-frequency electroencephalographic oscillations correlate with outcome of epilepsy surgery. Ann Neurol. 67, 209–20. [PubMed: 20225281]

Jefferys JG, et al., 2012 Mechanisms of physiological and epileptic HFO generation. Prog Neurobiol. 98, 250–64. [PubMed: 22420980]

Jiruska P, et al., 2017 Update on the mechanisms and roles of high-frequency oscillations in seizures and epileptic disorders. Epilepsia. 58, 1330–1339. [PubMed: 28681378]

Jozwiak S, et al., 2017 WONOEP appraisal: Development of epilepsy biomarkers-What we can learn from our patients? Epilepsia. 58, 951–961. [PubMed: 28387933]

Kerber K, et al., 2014 Differentiation of specific ripple patterns helps to identify epileptogenic areas for surgical procedures. Clin Neurophysiol. 125, 1339–45. [PubMed: 24368032]

Kerber K, et al., 2013 High frequency oscillations mirror disease activity in patients with focal cortical dysplasia. Epilepsia. 54, 1428–36. [PubMed: 23899121]

Lasztoczi B, et al., 2009 Synchronization of GABAergic inputs to CA3 pyramidal cells precedes seizure-like event onset in juvenile rat hippocampal slices. J Neurophysiol. 102, 2538–53. [PubMed: 19675286]

Le Van Quyen M, et al., 2008 Cell type-specific firing during ripple oscillations in the hippocampal formation of humans. J Neurosci. 28, 6104–10. [PubMed: 18550752]

Le Van Quyen M, et al., 2006 The dark side of high-frequency oscillations in the developing brain. Trends Neurosci. 29, 419–427. [PubMed: 16793147]

Lerner JT, et al., 2009 Assessment and surgical outcomes for mild type I and severe type II cortical dysplasia: a critical review and the UCLA experience. Epilepsia. 50, 1310–1335. [PubMed: 19175385]

Librizzi L, et al., 2017 Interneuronal Network Activity at the Onset of Seizure-Like Events in Entorhinal Cortex Slices. J Neurosci. 37, 10398–10407. [PubMed: 28947576]

Menendez de la Prida L, Trevelyan AJ, 2011 Cellular mechanisms of high frequency oscillations in epilepsy: on the diverse sources of pathological activities. Epilepsy Res. 97, 308–17. [PubMed: 21482073]

Mercer A, et al., 2006 Electrical coupling between pyramidal cells in adult cortical regions. Brain Cell Biol. 35, 13–27. [PubMed: 17940910]

Michalikova M, et al., 2017 Spikelets in Pyramidal Neurons: Action Potentials Initiated in the Axon Initial Segment That Do Not Activate the Soma. PLoS Comput Biol. 13, e1005237. [PubMed: 28068338]

Nariai H, et al., 2011a Ictal high-frequency oscillations at 80-200 Hz coupled with delta phase in epileptic spasms. Epilepsia. 52, e130–4. [PubMed: 21972918]

Nariai H, et al., 2011b Statistical mapping of ictal high-frequency oscillations in epileptic spasms. Epilepsia. 52, 63–74. [PubMed: 21087245]

Pinato G, Midtgaard J, 2005 Dendritic sodium spikelets and low-threshold calcium spikes in turtle olfactory bulb granule cells. J Neurophysiol. 93, 1285–94. [PubMed: 15483062]

Salamon N, et al., 2008 FDG-PET/MRI coregistration improves detection of cortical dysplasia in patients with epilepsy. Neurology. 71, 1594–601. [PubMed: 19001249]

Shiri Z, et al., 2015 Interneuron activity leads to initiation of low-voltage fast-onset seizures. Ann Neurol. 77, 541–6. [PubMed: 25546300]

Staba RJ, Bragin A, 2011 High-frequency oscillations and other electrophysiological biomarkers of epilepsy: underlying mechanisms. Biomark Med. 5, 545–56. [PubMed: 22003903]

van‘t Klooster MA, et al., 2015 Residual fast ripples in the intraoperative corticogram predict epilepsy surgery outcome. Neurology. 85, 120–8. [PubMed: 26070338]

van ‘t Klooster MA, et al., 2017 Tailoring epilepsy surgery with fast ripples in the intraoperative electrocorticogram. Ann Neurol. 81, 664–676. [PubMed: 28380659]

Vigmond EJ, et al., 1997 Mechanisms of electrical coupling between pyramidal cells. J Neurophysiol. 78, 3107–16. [PubMed: 9405530]

Weiss SA, et al., 2019 “Interneurons and principal cell firing in human limbic areas at focal seizure onset”. Neurobiol Dis. 124, 183–188. [PubMed: 30471414]

Wu JY, et al., 2010a Noninvasive testing, early surgery, and seizure freedom in tuberous sclerosis complex. Neurology. 74, 392–8. [PubMed: 20124204]

Wu JY, et al., 2010b Removing interictal fast ripples on electrocorticography linked with seizure freedom in children. Neurology. 75, 1686–94. [PubMed: 20926787]

Wu JY, et al., 2006 Magnetic source imaging localizes epileptogenic zone in children with tuberous sclerosis complex. Neurology. 66, 1270–2. [PubMed: 16636252]

Ye H, Kaszuba S, 2017 Inhibitory or excitatory? Optogenetic interrogation of the functional roles of GABAergic interneurons in epileptogenesis. J Biomed Sci. 24, 93. [PubMed: 29202749]

Zsiros V, Maccaferri G, 2005 Electrical coupling between interneurons with different excitable properties in the stratum lacunosum-moleculare of the juvenile CA1 rat hippocampus. J Neurosci. 25, 8686–95. [PubMed: 16177037]

Highlights

- In pediatric epilepsy tissue samples, pathological high frequency oscillations (HFOs >250 Hz) are associated with increased spontaneous GABAergic synaptic activity.
- Pacemaker GABA activity (PGA) is also associated with pathological HFOs.
- Fast-spiking interneurons display signs of hyperexcitability exclusively in pathological HFO+ areas.
- These results suggest an active role of GABAergic interneurons in the generation of pathological HFOs.

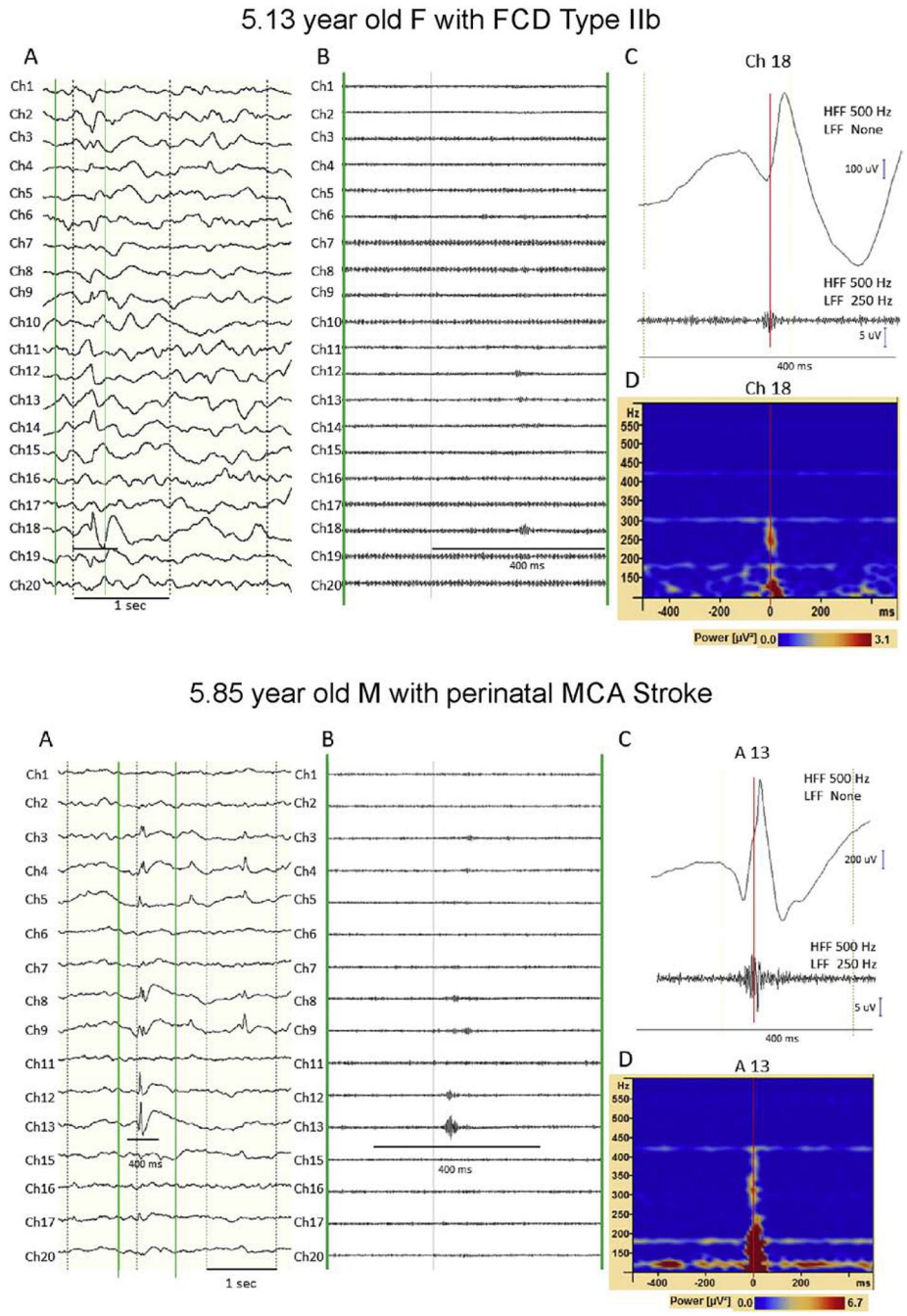

Figure 1:

ECoG recordings from two example cases, one with CD type IIb (upper panel) and the other with perinatal infarct (lower panel), showing the occurrence of pathological HFOs. **A.** Original ECoG trace with LFF 1.6Hz, HFF 500 Hz. **B.** Temporally expanded filtered ECoG trace for fast ripples (FRs). **C.** Further temporally expanded trace for a FR event with LFF off, HFF 500 Hz. **D.** Time-frequency plot for a FR event. Power change is shown as a function of time and frequency. An “island” of FR activity is observed between 250-500 Hz.

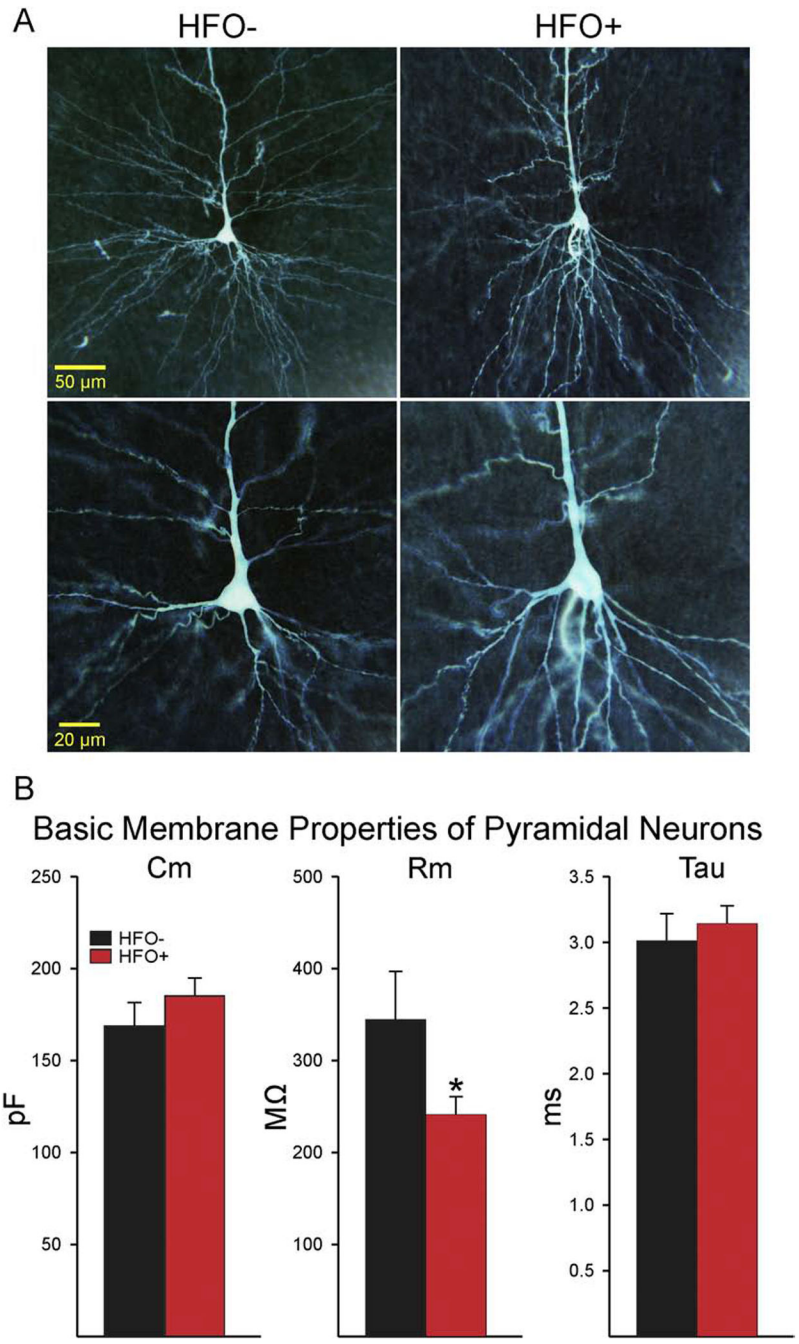

Figure 2:

A. Examples of biocytin-filled CPNs from HFO− and HFO+ areas (cells on the bottom panels are the same cells at higher magnification). Calibrations on the left apply to both panels. **B.** Bar graphs illustrate average (±SEM) basic membrane properties (Cm=cell capacitance, Rm=input resistance and Tau=decay time constant) of pyramidal neurons in HFO− and HFO+ areas. There was a significant reduction of membrane input resistance in neurons from HFO+ areas.

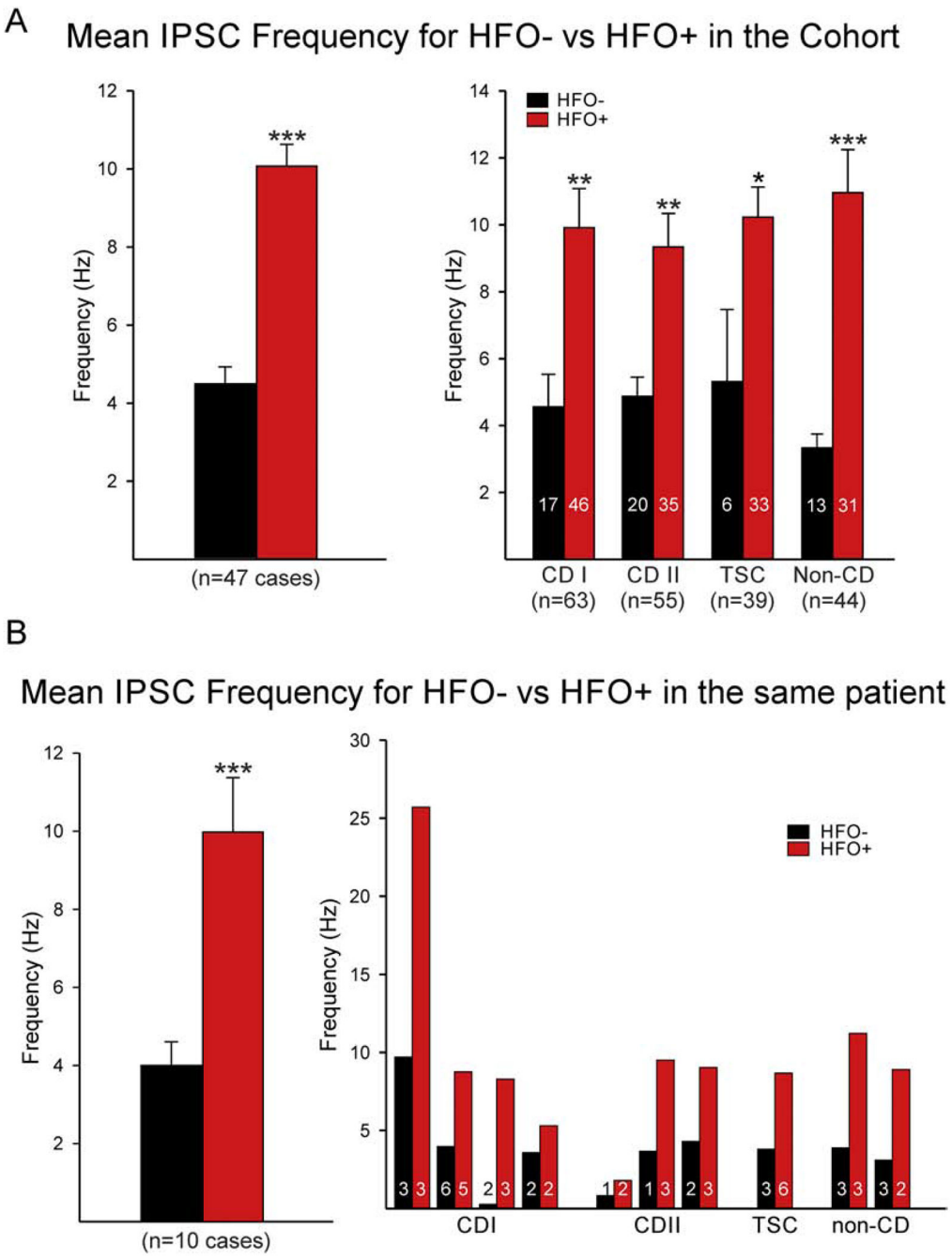

Figure 3:

A. Mean IPSC frequencies in all cases (HFO− versus HFO+) and separated by pathology. Regardless of pathology, HFO+ areas had significantly higher frequencies compared with HFO− areas. **B.** Graphical comparison of mean IPSC frequencies in 10 cases where HFO− and HFO+ could be obtained from the same patient (left). Comparison of IPSC frequencies in each patient and separated by pathology (4 CD type I, 3 CD type II, 1 TSC, and 2 non-CD cases). Numbers within bars in A and B (right panels) represent the number of cells recorded and used to compute the mean frequency shown in each bar graph.

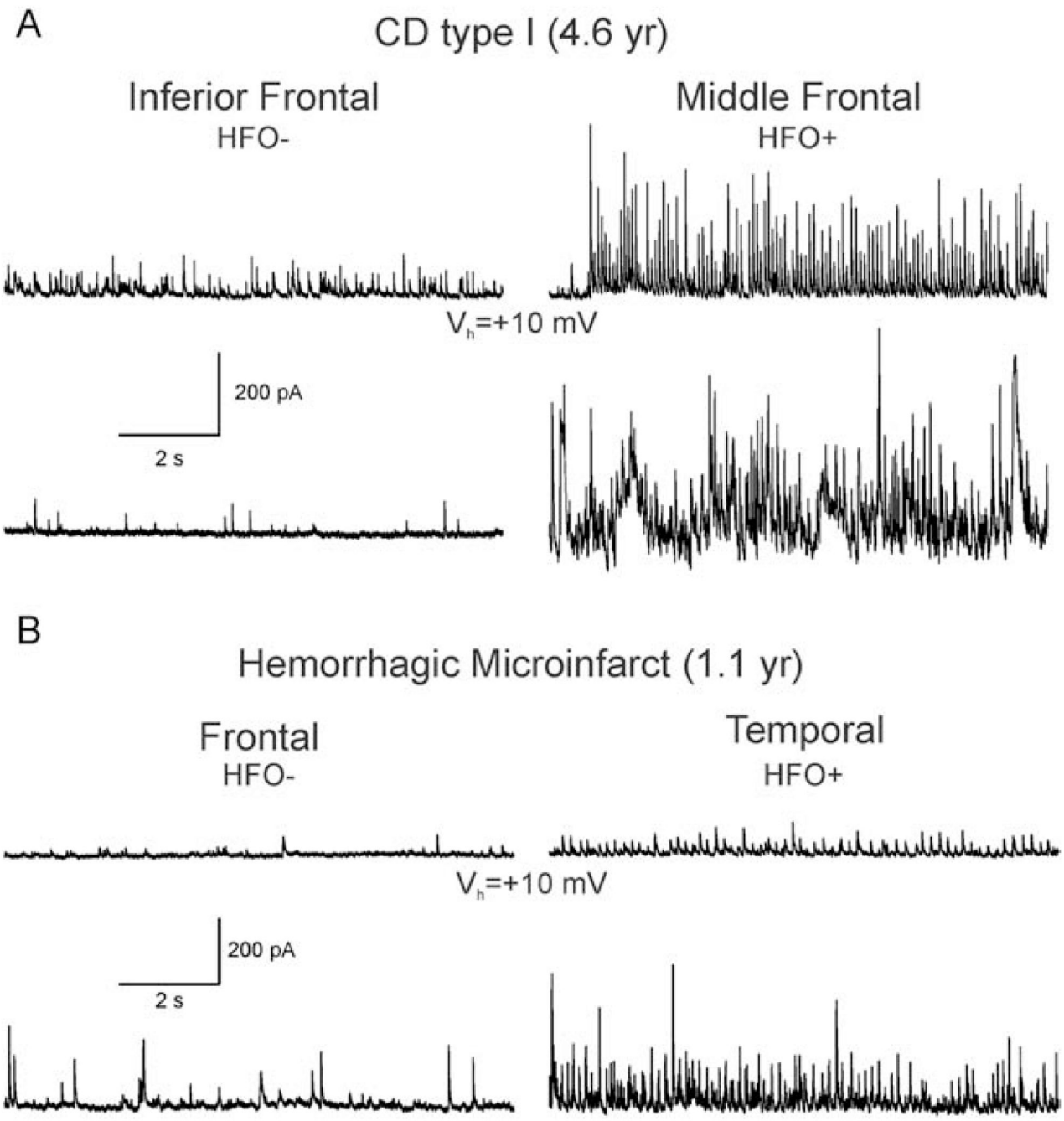

Figure 4:

In these two cases (**A.** CD type I and **B.** hemorrhagic infarct), cells in HFO+ areas displayed higher frequency of spontaneous GABA synaptic currents as well as PGA in 3 of them. In contrast, cells in the HFO− area displayed low activity and no PGA.

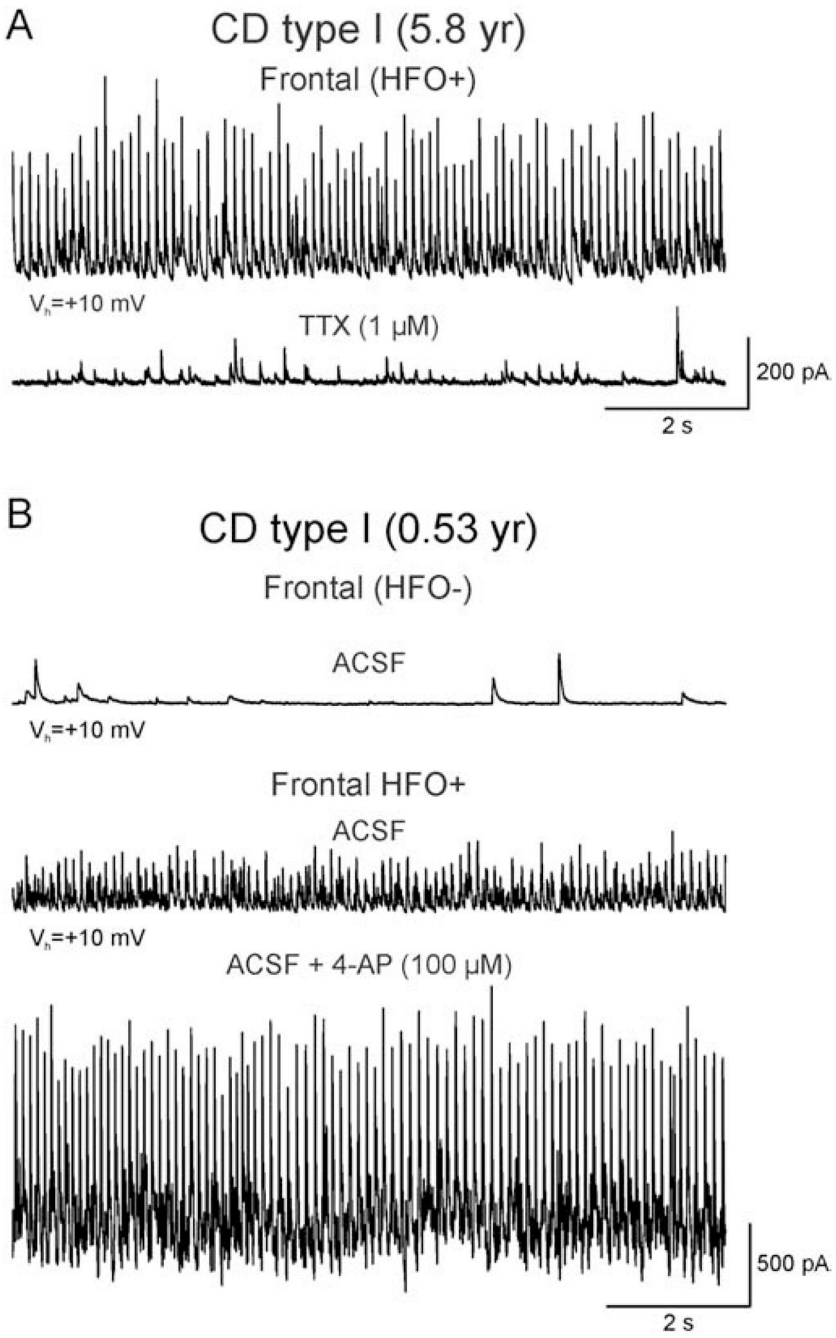

Figure 5:

PGA activity was observed in these CD type I cases. Increased frequency of sIPSCs as well as PGA was dependent on action potentials as after addition of TTX **(A)** there was a dramatic decrease in activity. In addition, 4-AP exacerbated the amplitude of PGA **(B)**.

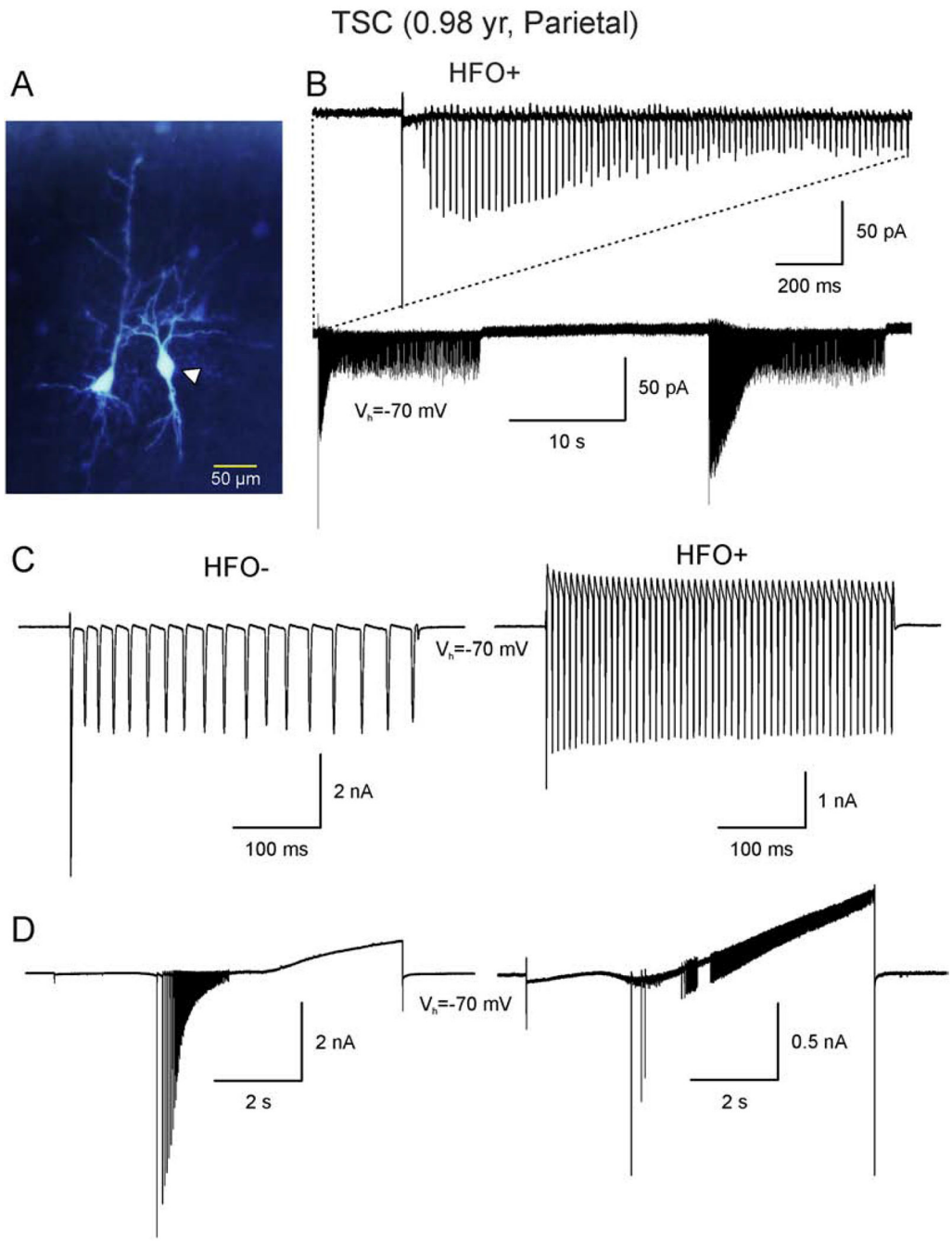

Figure 6:

Interneuron activity was increased in HFO+ areas. **A.** Panel shows one pyramidal neuron and one interneuron (arrowhead) recorded sequentially. **B.** Based on intrinsic membrane properties and firing pattern, this cell was classified as FSI (putative parvalbumin-expressing interneurons). FSIs in HFO+ areas displayed signs of hyperexcitability manifested by increased firing frequency after application of a depolarizing step voltage command from V_{hold} = −70 mV to −30 mV **(C)** or a slow depolarizing ramp voltage command **(D)**.

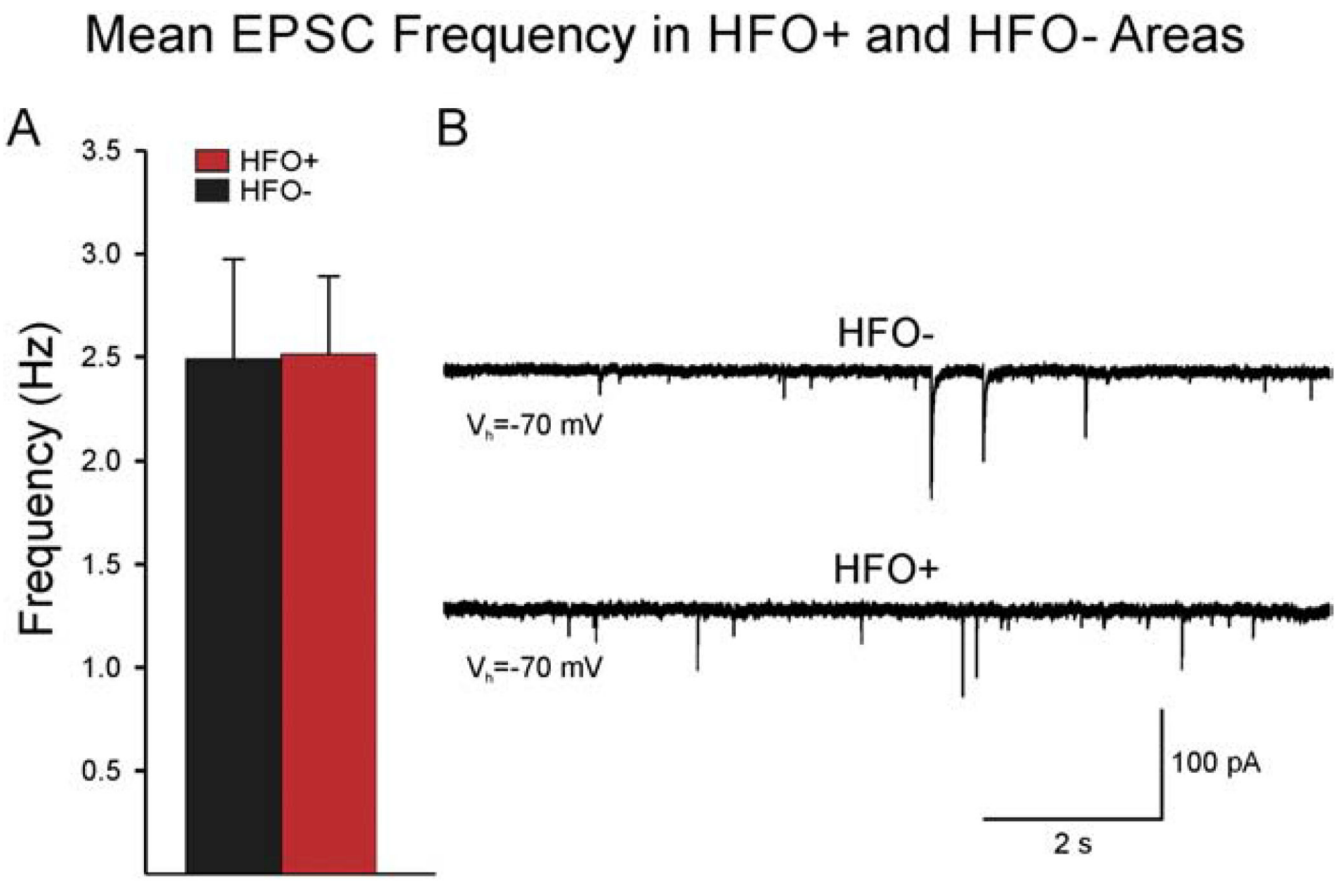

Figure 7:

Excitatory post-synaptic activity was almost identical in pyramidal neurons from HFO− versus HFO+ areas. **A.** Graph shows frequency of spontaneous synaptic activity recorded at −70 mV. **B.** Example traces of spontaneous synaptic currents recorded in CPNs from HFO− and HFO+ areas.

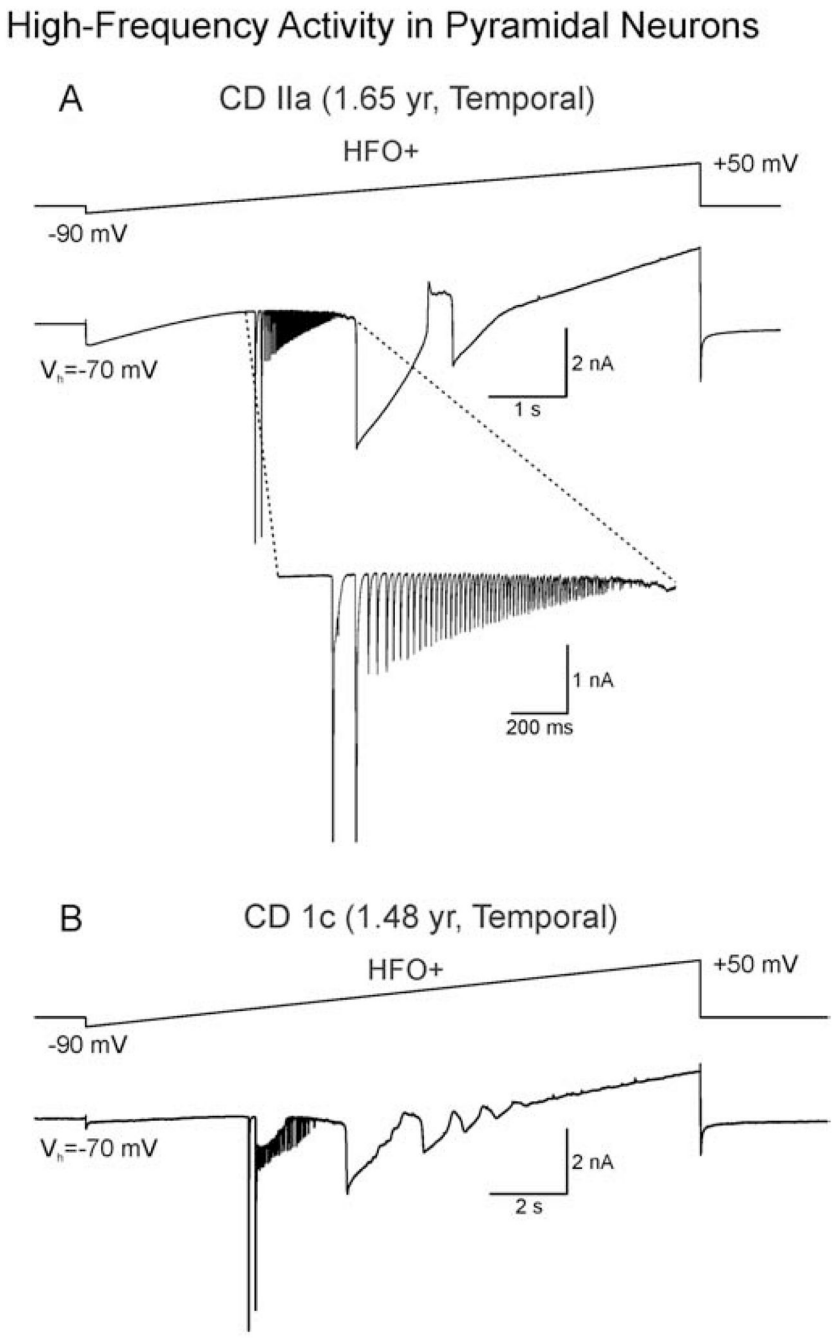

Figure 8:

High-frequency spikelets were observed in some pyramidal neurons in HFO+ areas when the cell was depolarized with a slow ramp voltage command. In **A** high frequency spikelets followed 2 full-blown action potentials whereas in **B** the spikelets were superimposed on an unclamped Ca^{2+} spike.

Table I.

Cohort

Pathology	n	Mean Age (yr) (range)	Gender	# Cells	HFO+	HFO−
CD Type I	13	2.8±0.8 (0.53-7.48)	10M 3F	63	46	17
CD Type II	15	3.4±0.9 (0.22-9.22)	6M 9F	55	35	20
TSC	10	2.2±0.7 (0.87-6.1)	8M 2F	39	33	6
Non-CD	9	4.8±1.7 (1.07-9.99)	4M 5F	44	31	13
Total	**47**	**3.3±1.7 (0.22-9.99)**	**28M 19F**	**201**	**145**	**56**

Table II.

Basic Membrane Properties of Cortical Interneurons

	Capacitance (pF)	Input Resistance (MΩ)	Tau (ms)
HFO+ (n=28)	43.7±3.8	557.2±82.4	0.79±0.09
HFO− (n=7)	42.7±4.1	757.5±393.9	0.63±0.2